J Mater Sci (2008) 43:3664–3669
DOI 10.1007/s10853-008-2586-1

MWNTs/PANI composite materials prepared by in-situ chemical oxidative polymerization for supercapacitor electrode

Ling-Bin Kong · Jing Zhang · Jing-Jing An · Yong-Chun Luo · Long Kang

Received: 29 December 2007 / Accepted: 6 March 2008 / Published online: 23 March 2008

Abstract Multi-walled carbon nanotubes (MWNTs)/polyaniline (PANI) composite materials were prepared by in-situ chemical oxidative polymerization of an aniline solution containing well-dispersed MWNTs. The supercapacitive behaviors of these composite materials were investigated with cyclic voltammetry (CV), charge–discharge tests, and ac impedance spectroscopy, respectively. The composites based on the charge-transfer complex between well-dispersed MWNTs and PANI matrixes show much higher specific capacitance, better thermal stability, lower resistance, and were more promising for applications in supercapacitors than a pure PANI electrode. The highest specific capacitance value of 224 Fg^{-1} was obtained for the MWNTs/PANI composite materials containing MWNTs of 0.8 wt%. The improvement mechanisms of the capacitance of the composite materials were also discussed in detail.

Introduction

Carbon nanotubes (CNTs) have been widely studied as fillers for polymeric composites due to their extremely high strength, stiffness, and flexibility [1–3]. It has been demonstrated experimentally that the introduction of CNTs into a polymer matrix improves the electrical conductivity as well as the mechanical properties of the original polymer matrix [4–6]. As a result, CNTs-based functional materials have become popular subjects of study in recent years. Many attempts have been devoted to the use of conducting polymers as electrode materials in electrochemical capacitors, often called supercapacitors [7–10]. Based on these studies, the conducting polymers-coated CNTs might prove to be an even more promising material.

Among various conducting polymers, polyaniline (PANI) has potential uses in synthesizing conducting CNTs/polymers owing to its environmental stability, good processability, and reversible control of conductivity both by protonation and by charge-transfer doping [11–13]. Recently, the studies of designing and preparing CNTs/PANI composites have been made rapidly progress [14–15], for example, the doped Multi-walled carbon nanotubes (MWNTs)/PANI composites prepared with or without protonic acid synthesized via in-situ polymerization [16]; CNTs/PANI composites by electrochemical [17–19]; and microemulsion [20] polymerization showed good electrochemical properties; functional MWNTs/PANI composite films have been prepared by chemical method as a promising support material improves the electrocatalytic activity for formic acid oxidation greatly [21]. Some related work has been done on composites of MWNTs coated with PANI. However, there is less reported on fabricating MWNTs/PANI composites by in-situ chemical oxidative polymerization of an aniline solution containing well-dispersed MWNTs and further characterizing on the supercapacitive behavior of the composites.

The study by Sun et al. has shown that CNTs can be dispersed in aniline via formation of a donor–acceptor complex. The solubility of SWNTs in aniline is up to 8 mg ml^{-1} [22]. Based on this work, here we choosed MWNTs which are easier to purify and has lower cost than SWNTs and used the above-mentioned method to obtain the well-dispersed MWNTs-aniline solution and prepared the MWNTs/PANI composites via an chemical oxdative

L.-B. Kong (✉) · J. Zhang · J.-J. An · Y.-C. Luo · L. Kang
State Key Laboratory of Gansu Advanced Non-ferrous Metal Materials, Lanzhou University of Technology, Lanzhou 730050, P.R. China
e-mail: konglb@lut.cn

polymerization. The results revealed that the MWNTs/PANI composites show much higher specific capacitance, better thermal stability, lower resistance, and more promise for applications in supercapacitors than a pure PANI electrode. The highest specific capacitance value of 224 Fg^{-1} was obtained for the MWNTs/PANI composites containing MWNTs of 0.8 wt%. Scanning electron microscopy (SEM), Fourier transform infrared (FTIR) spectroscopy, thermogravimetric analysis (TGA), and electrochemical impedance spectroscopy (EIS) were applied to reveal the improvement mechanisms of supercapacitive characteristic of the MWNTs/PANI composites.

Experimental methods

The MWNTs were obtained from Tsinghua-Nafine Nano-Power Commercialization Engineering Center (the purity of the pristine MWNTs was 99% and 10 nm diameter). MWNTs were treated using a 3:1 mixture of concentrated H_2SO_4/HNO_3 prior to the experiments as described in a previous investigation [23]. In a typical synthesis experiment, 0, 0.2, 0.4, 0.8 wt% of MWNTs (weight percent with respect to aniline monomer) were dissolved in aniline and were heated at reflex for 5 h in the dark. The refluxing solution of the colorless aniline first became brownish and then turned dark, indicating that MWNTs have been dissolved well into aniline. After being cooled to room temperature, MWNTs-aniline solutions were obtained by filtration through 0.1-μm-diameter Supor Membrane disk filters (Gelman).

The composite of protonic acid doped PANI with MWNTs was synthesized via in-situ chemical oxidation polymerization. Then a solution of 2 M HCl containing 0.5 M aniline dissolved MWNTs was stirred at 0–5 °C and then an equal volume of pre-cooled (5 °C) oxidant solution containing 0.2 M ammonium persulfate (APS) was slowly added to the above solution for 1 h. The reaction mixture left for polymerization with constant mechanical stirring at a reaction temperature of 0–5 °C for a further 2 h and then resulting green suspension, indicating the formation of PANI. The MWNTs/PANI composites were obtained by filtering and rinsing the reaction mixtures with deionized water followed by drying under vacuum at 60 °C for 24 h.

The mixture containing 85 wt% MWNTs/PANI composites, 5 wt% acetylene black, 5 wt% graphite, and 5 wt% polytetrafluoroethylene (PTFE) was well mixed, and then pressed onto a Ni-foam current collector (area was 1 cm^2). The electrochemical performances of the prepared electrodes were characterized by cyclic voltammetry (CV) recorded from −0.20 to 0.80 V at 5 $mVs^{-1}$and charge–discharge tests were performed at different constant current densities, with cutoff voltage of −0.20 to 0.80 V. EIS measurements for the MWNTs/PANI composite electrode were performed under open circuit potential in an ac frequency range from 100,000 to 0.01 Hz with an excitation signal of 5 mV. The used electrolyte was 1 M $NaNO_3$ solution. The experiments were carried out using a beaker-type electrochemical cell, in which platinum and the saturated calomel electrode (SCE) are used as counter and reference electrodes. The electrode performances were all measured on CHI660C electrochemical work station at room temperature (25 °C).

The morphology and microstructure of the MWNTs/PANI composites were characterized using SEM (Model JSM-6701F, Japan). TGA data were obtained by a Thermogravimetric Analyzer (Netzsch, STA-449C, Germany). The IR spectra were recorded by using a FTIR spectrometer (Nexus670, USA). Conductivity of all samples (25 mm in diameter and 0.7 ~ 0.8 mm thick) were measured at room temperature by a four-probe method (SDY-4, China).

Results and discussion

Figure 1 illustrates the formation mechanism of the MWNTs/PANI composites via in-situ chemical oxidative polymerization. The surface of MWNTs can be treated with a mixture of concentrated H_2SO_4 and HNO_3 to produce carboxylic acid groups at local defect sites of MWNTs, and to increase the solubility of MWNTs in aniline monomer. The interaction between MWNTs and the aniline monomer, as well as is the carboxyl groups of MWNTs and the amino groups of aniline monomers. Such strong interaction ensures that the aniline monomer is adsorbed on the surface of MWNTs, which serve as the core and self-assembly template during the formation of the tubular nanostructure. The further investigation can be seen from SEM micrographs of the pure PANI and the MWNTs/PANI composites, as shown in Fig. 2, respectively. As can be seen from Fig. 2a, the pure PANI showed

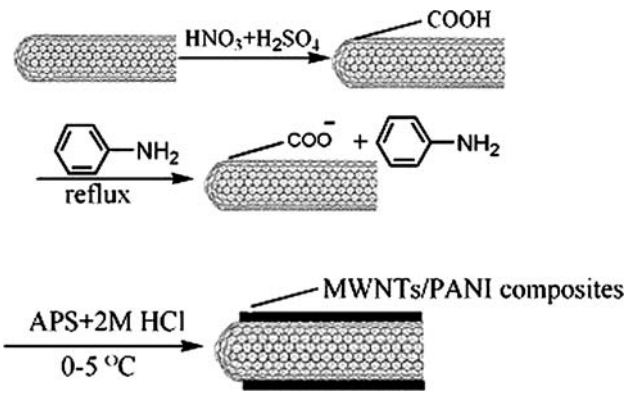

Fig. 1 Schematic procedure for the preparation of MWNTs/PANI composites

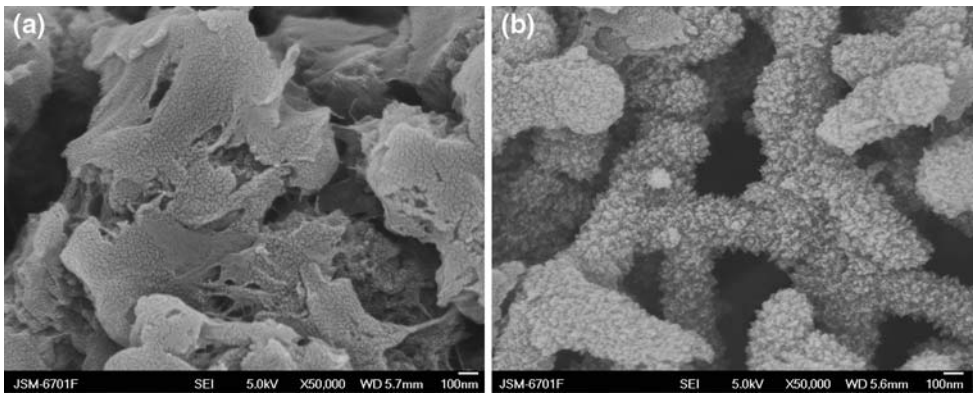

Fig. 2 SEM images of (**a**) the pure PANI, and (**b**) the MWNTs/PANI composite with 0.8 wt% MWNTs

a drastic loss of porosity, but a sheet texture, such texture has less active sites for faradic reaction and does not facilitate the charge-transfer for the electrode materials. By contrast, from Fig. 2b, it can be seen that all polymer is dispersed on the nanotubes, which indicates that the MWNTs were well dispersed in the composites, and keeping the advantage of the entangled network of the nanotubes that allows a good access of the electrolyte to the active polymer material. There is no doubt that such texture of the capacitor electrodes is optimal for the fast ion diffusion and migration in the polymer which can increase more active sites of the composite for faradic reaction and larger specific capacitance than pure PANI, so that the composite electrode performance are improved. We carried out the following experiments to investigate the effect of the MWNTs on the electrochemical properties and capacitance performance of the composite.

Thermal stability testing was conducted using a thermogravimetric analyzer (TGA). Figure 3 showed a comparison of mass loss in PANI and the MWNTs/PANI composites with 0.8 wt% MWNTs upon heating in a nitrogen atmosphere. A rapidly mass decrease was found for pure PANI in the temperature range between 500 and 600 °C, while the MWNTs/PANI composite is not obvious. The total mass loss up to 800 °C was estimated to be about 79% and 62% for PANI and the MWNTs/PANI composites, respectively. The trend in the degradation curve of the MWNTs/PANI composites was similar to that of PANI, we can see that the degradation of the MWNTs/PANI composite was mainly controlled by PANI, but the thermal stability of PANI in the composites is somewhat better compared with the pure PANI.

Figure 4 shows the FTIR spectra for the pure PANI and the MWNTs/PANI composites with 0.8 wt% MWNTs. The both spectra exhibit the clear presence of benzoid and quinoid ring vibrations at 1,500 and 1,600 cm^{-1}, respectively, thereby indicating observed for PANI. As commonly observed for PANI, the quinoid band at 1,600 cm^{-1} is less intense than that of the benzenoid band at 1,500 cm^{-1}. The very weak and broad band near

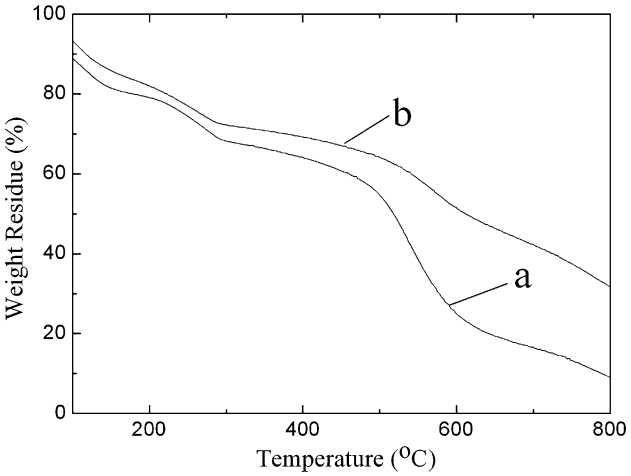

Fig. 3 TGA data of pure PANI (**a**), and MWNTs/PANI composites with 0.8 wt% MWNTs (**b**) measured under a nitrogen atmosphere at room temperature

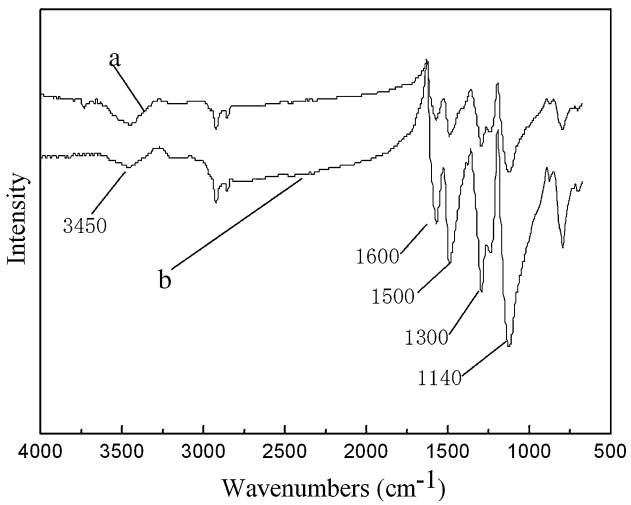

Fig. 4 FTIR spectra of the pure PANI (**a**), and MWNTs/PANI composites with 0.8 wt% MWNTs (**b**)

3,450 cm^{-1} corresponds to the stretching of the N–H bonds; the band at 1,300 cm^{-1} is assigned to the stretching of the C–N bonds of the aromatic amines. The absorption

at 1,140 cm^{-1} was described as the "electronic-like band" and is considered to be a measure of the degree of delocalization of electron and thus it is characteristic peak of PANI conductivity [24].

There are two differences from the two FTIR spectra, one is that the absorption at 1,140 cm^{-1} of the MWNTs/PANI composites is stronger than that of the pure PANI. It appears that the intensity of this peak increased with the introduction of MWNTs, which agrees well with our conductivity measurements. This fact may suggest that the strong interaction between MWNTs and PANI facilitates the effective degree of electron delocalization, and thus enhances the conductivity of the polymer chains. Another is the absorption near 3,450 cm^{-1} for the N–H stretching region is apparent in the pure PANI yet not clear in the composites. Owing to the introduction of MWNTs, the peak intensity decreased, this may be ascribed to that the MWNTs sp^2 carbons compete with the chloride ion and thus perturb the H-bonding environment and increase the N–H stretch intensity [16].

The voltammetric responses are employed to evaluate the electrochemical characteristics of the electrode materials. Figure 5 shows the cyclic voltammograms (CVs) of pure PANI (a) and the MWNTs/PANI composites with 0.8 wt% MWNTs (b). Both curves show no obvious peak found on both positive and negative sweeps of every electrode in the whole potential range. Moreover, both CVs with respect to the zero-current line and a rapid current response on voltage reversal at each end potential, as well as the rectangular-like and almost symmetric *I–E* responses of ideal capacitive behavior can be observed; but for pure PANI and the composites, although the symmetric and the rectangular-like characteristic of ideal *I–E* responses are not so markedly, they also show the capacitive-like characteristics in the neutral medium $NaNO_3$ solution. It can be seen that the output current of the composites is much larger than that of pure PANI. Since capacitance can be estimated from the output current divided by the scan rate, this indicates that the specific capacitance of the composites is larger than that of pure PANI. This improvement of the capacitance for the MWNTs/PANI composites may be due to the high-surface area and good conductivity of MWNTs. However, an accurate capacitance value should be obtained from the constant charge–discharge experiments.

Typical constant charge–discharge responses for pure PANI and the MWNTs/PANI composites with 0.2, 0.4, 0.8 wt% MWNTs at 0.5 A/g are shown as Fig. 6. On the four curves, the *E–t* responses of the anodic charge process show the mirror image of their corresponding cathodic discharge counterparts. From these we can see that the PANI and MWNTs/PANI composites polymerized here exhibit the ideally capacitive behavior in 1 M $NaNO_3$ solutions. The average specific capacitance of both electrodes can be obtained from these curves by the following relationship, i.e., $SC = I\Delta t/\Delta Em$. Here, I is the discharge current, Δt is the discharge time corresponding to the voltage difference (ΔE), and m is the active electrode mass. On the basis of the above equation, the average specific pseudocapacitance for PANI is 178 Fg^{-1} at a discharge current density of 0.5 $Ag^{-1}$and for the MWNTs/PANI composites are 200.5, 205, and 224 Fg^{-1}, respectively. Figure 6 shows the composite has a larger capacitance than that of the pure PANI, even if the content of MWNT is only 0.8 wt%. The highly accessible surface area and low resistivity of the CNT itself will improve the contact between PANI matrixes; moreover, the well-coated MWNT made the composites a porous morphology, formed by enlacing the PANI-coated tubes together in a nanoporous three-dimensional network, which may provide

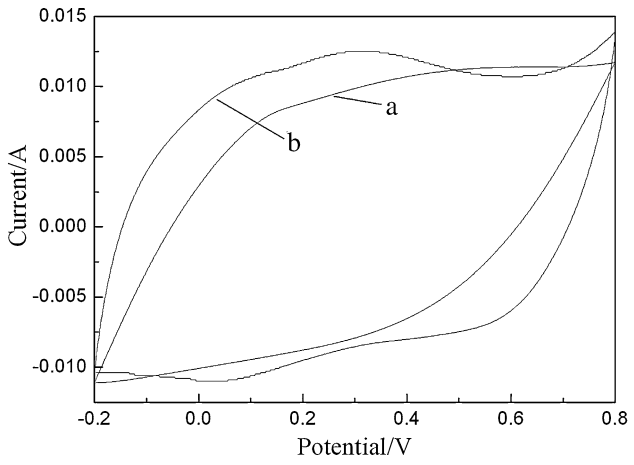

Fig. 5 Cyclic voltammograms of pure PANI (**a**), MWNTs/PANI composites with 0.8 wt% MWNTs (**b**). Scan rate: 5 mV/s. Current density: 0.25 A/g

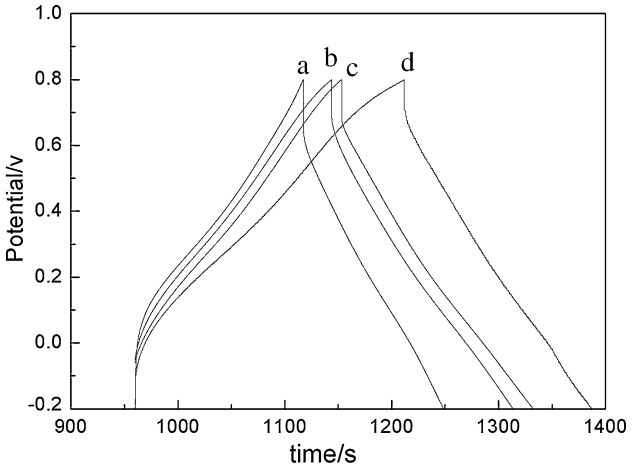

Fig. 6 Galvanostatic charge–discharge curves of pure PANI (**a**), MWNTs/PANI composites with 0.2 (**b**), 0.4 (**c**), 0.8 wt% (**d**) MWNTs. Current density: 0.5 A/g

a large surface area and allow excellent electrolyte access and storage in three dimensions. These, overall, make available the composite more active sites for faradic reaction and larger specific capacitance than pure PANI.

Figure 7 shows the variation of specific capacitance with discharge current density for the pure PANI and the MWNTs/PANI composites. It can be seen that the composites electrodes have a consistent higher specific capacitance than pure PANI, although the specific capacitance of pure PANI and MWNTs/PANI composite electrodes all decrease gradually with the increasing discharge current density. But comparing to pure PANI, the capacitance-decreasing rate with increasing discharge current density for the MWNTs/PANI composites is lower. This point can be more obviously seen from Fig. 7, where, for pure PANI electrode, the specific capacitance at a discharge current density of 5 Ag^{-1} drops by about 90% from that at 0.25 Ag^{-1}, while the capacitance of MWNTs/PANI composites electrode drops only by about 73%, 68%, 61%. The rapid deterioration of specific capacitance of the pure PANI electrode may be caused by the large internal resistance of the electrode, which causes a large ohmic drop at high-discharging current density and results in the rapid decrease of the specific capacitance and power density. The uniform dispersion CNTs adhere strongly to the PANI matrix by the formation of a charge-transfer complex rather than the weak van der waals interaction between them, which causes a small ohmic drop at high-discharging current density and makes the decrease of the specific capacitance and power density slower. To prove such a standpoint, we carried out the ac impedance measurements.

The principal objective of the EIS experiments is to gain the interfacial properties (capacitance, electron-transfer resistance) of electrodes. The complex impedance can be presented as the sum of the real, Z′, and imaginary, Z″ components that originate mainly from the resistance and capacitance of the cell, respectively. A typical shape of an electrochemical impedance spectrum (presented in the form of a Nyquist plot) includes a semicircle region lying on the Z′-axis followed by a straight line. The semicircle portion, observed at higher frequencies, corresponds to the electron-transfer-limited process, whereas the linear part is characteristic of the lower frequencies range and represents the diffusional-limited electron-transfer process [25]. It is well known that CNTs can be well dispersed in aniline via the formation of a donor–acceptor complex. So the dependence of impedance spectra of the conducting polymer composites may be considered for investigating the characteristics of composites structures and ion transport in the MWNTs/PANI composites interface and PANI/electrolyte interface. From Fig. 8, we can see the impedance spectra of the MWNTs/PANI composites with 0, 0.2, 0.4, 0.8 wt% MWNTs are similar in form, composed of a single semicircle in high-frequency and straight line in the low-frequency region. As the content of MWNTs increased, the diameters of the four semicircles greatly decline, that is attributed to the transport of electrons and the charge-transfer resistance of the MWNTs/PANI composites is much lower than that of the pure PANI. It is further proved that the formation of the charge-transfer complex between the uniform dispersion MWNTs and the PANI matrix of the composites, which results in enhanced doping degree, lowers defect density, lowers the resistance, and facilitates the charge-transfer of the composites.

From the frequency (f_0) corresponding to the maximum of the imaginary component (Z″) of the semicircle, the time constant (Γ) of every electrode can be calculated using Eq. 1

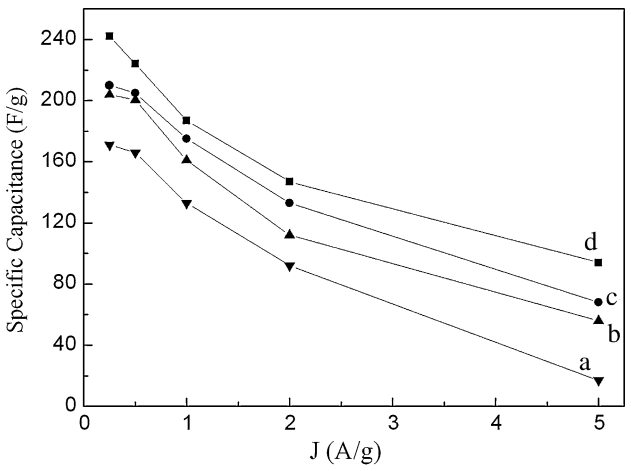

Fig. 7 Specific capacitance of pure PANI (**a**), MWNTs/PANI composites with 0.2 (**b**), 0.4 (**c**), 0.8 wt% (**d**) MWNTs at the different current density

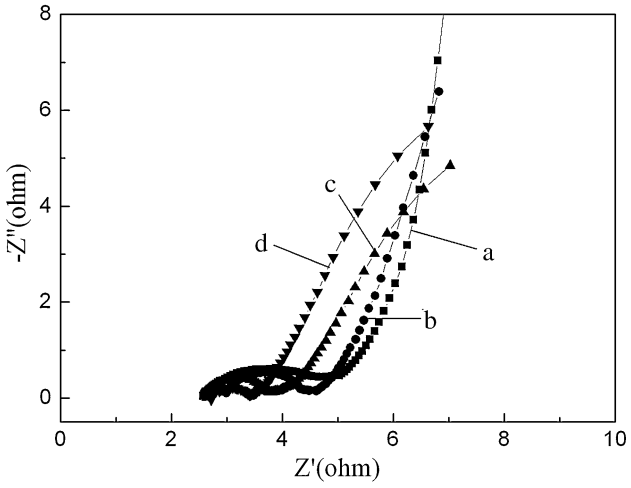

Fig. 8 Impedance Nyqyist plots of PANI and MWNTs/PANI composites electrode with different contents of MWNTs: 0 (**a**), 0.2 (**b**), 0.4 (**c**), 0.8 wt% (**d**)

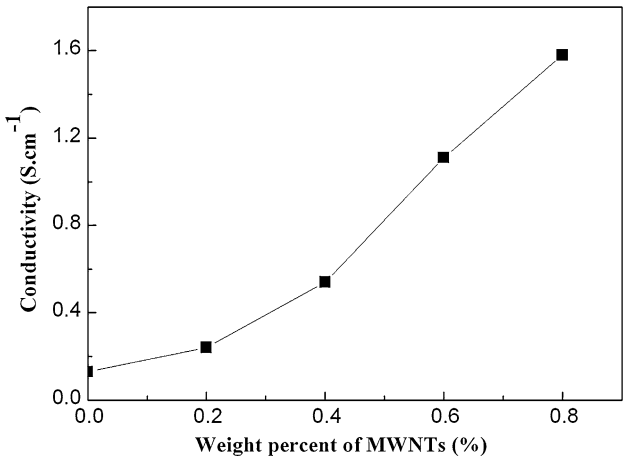

Fig. 9 Conductivity of the MWNTs/PANI composites electrode with different contents of MWNTs: 0, 0.2, 0.4, 0.8 wt%

$$\Gamma = 1/(2\pi f_0) \quad (1)$$

The values of Γ obtained from Fig. 8 are 0.195 ms for PANI (a), 0.074 ms (b), 0.063 ms (c), and 0.048 ms (d) for MWNTs/PANI composite films, respectively. The lower Γ-value of MWNTs/PANI is preferred for electrochemical capacitor for fast charge–discharge processes [26].

In Fig. 9, we present the conductivity data measured according to the standard four-point probe technique at room temperature. The conductivity of MWNTs/PANI composites increased rapidly from 1.31×10^{-1} to 1.58 S cm^{-1} as the MWNTs content ranging from 0 to 0.8 wt%. The combination of PANI, with MWNTs, had effectively increased the conductivity of the MWNTs/PANI composites, which is nearly 12 times higher than that of the pure PANI. This may also be attributed to the doping effect associated with MWNTs which were believed to help induce the formation of a more efficient matrix for charge transport, thus enhancing the conductivity of the MWNTs/PANI composites.

Conclusions

The MWNTs/PANI composite materials were synthesized successfully by in-situ chemical oxidative polymerization of aniline containing well-dispersed MWNTs. Microstructure of MWNTs/PANI composite materials show that the MWNTs were well dispersed in the composites. Owing to the presence of MWNTs, the MWNTs/PANI composite electrodes showed better thermal stability, higher conductivity, lower resistance, better capacitive characteristics than the pure PANI electrode. The specific capacitance of 224 Fg^{-1} obtained for MWNTs/PANI composites with only 0.8 wt% MWNTs is larger than 178 Fg^{-1} of the pure PANI.

Acknowledgements The authors acknowledge the financial support by the National Natural Science Foundation of China (No. 50602020) and the National Basic Research Program of China (No. 2007CB216408).

References

1. Iijima S, Ichihashi T (1993) Nature 363:603. doi:10.1038/363603a0
2. Niu CM, Sichel EK, Hoch R, Moy D, Tennent H (1997) Appl Phys Lett 70:1480. doi:10.1063/1.118568
3. Yu MF, Files BS, Arepalli S, Ruoffet S (2000) Phys Rev Lett 84:5552. Medline. doi:10.1103/PhysRevLett.84.5552
4. Schadler LS, Giannaris SC, Ajayan PM (1998) Appl Phys Letts 73:3842. doi:10.1063/1.122911
5. Wagner HD, Lourie O, Feldman Y, Tenne R (1998) Appl Phys Lett 72:188. doi:10.1063/1.120680
6. Qian D, Dickey EC, Andrews R, Rantell T (2000) Appl Phys Letts 76:2868. doi:10.1063/1.126500
7. Conway BE (1999) Electrochemical supercapacitors. Kluwer Academic/Plenum Publishers, New York
8. Conway BE (1991) J Electrochem Soc 138:1539. doi:10.1149/1.2085829
9. Gupta V, Miura N (2006) J Power Sources 157:616. doi:10.1016/j.jpowsour.2005.07.046
10. Gupta V, Miura N (2006) Electrochim Acta 52:1721. doi:10.1016/j.electacta.2006.01.074
11. Skotheim TA, Elsenbaumer RL, Reynolds JR (1997) Handbook of conducting polymers. Marcel Dekker, New York
12. Konyushenko EN, Stejskal J, Trchova M, Hradil J, Kovarova J, Prokes J, Cieslar M, Hwang JY, Chen KH, Sapurina I (2006) Polymer 47:5715. doi:10.1016/j.polymer.2006.05.059
13. Premamoy G, Samir KS, Amit C (1999) Eur Polym J 35:699. doi:10.1016/S0014-3057(98)00157-8
14. Lefrant S, Baibarac M, Baltog I, Mevellec JY, Godon C Chauvet O (2005) Diam Relat Mater 14:867. doi:10.1016/j.diamond.2004.11.035
15. Maser WK, Benito AM, Callejas MA, Seeger T, Martínez MT, Schreiber J, Muszynski J, Chauvet O, Osváth Z, Koós AA, Biró LP (2003) Mater Sci Eng C 23:87. doi:10.1016/S0928-4931(02)00235-7
16. Zengin H, Zhou W, Jin J, Cserw R, Smith DW Jr, Echegoyen L, Carroll DL, Foulger SH, Ballato J (2002) Adv Mater 14:1480. doi:10.1002/1521-4095(20021016)14:20≤1480::AID-ADMA1480≥3.0.CO;2-O
17. Zhou Y-K, He B-L, Zhou WJ, Li H-L (2004) J Electrochem Soc 151:A1052. doi:10.1149/1.1758812
18. Li X-H, Wu B, Huang J-E, Zhang J, Liu Z-F, Li H-L (2003) Carbon 41:1670. doi:10.1016/S0008-6223(03)00124-6
19. Huang J-E, Li X-H, Xu J-C, Li H-L (2003) Carbon 41:2731. doi:10.1016/S0008-6223(03)00359-2
20. Barraza HJ, Pompeo F, O'Rear EA, Resasco DE (2002) Nano Lett 2:797. doi:10.1021/nl0256208
21. Zhu Z-Z, Wang Z, Li H-L (2008) Appl Surf Sci 254:2934
22. Sun Y, Wilson SR, Schuster DI (2001) J Am Chem Soc 123:5348. Medline. doi:10.1021/ja0041730
23. Li Q-W, Yan H, Cheng Y, Zhang J, Liu Z-F (2002) J Mater Chem 12:1179. doi:10.1039/b109763f
24. Quillard S, Louarn G, Lefrant S, MacDiarmid AG (1994) Phys Rev B 50:12496. doi:10.1103/PhysRevB.50.12496
25. Gamby J, Taberna PL, Simon P, Fauvarque JF, Chesneau M (2001) J Power Sources 101:109. doi:10.1016/S0378-7753(01)00707-8
26. Burke A (2000) J Power Sources 91:37. doi:10.1016/S0378-7753(00)00485-7